Bmpr2 Mutant Rats Develop Pulmonary and Cardiac Characteristics of Pulmonary Arterial Hypertension

Aurélie Hautefort, Pedro Mendes-Ferreira, Jessica Sabourin, Grégoire Manaud, Thomas Bertero, Catherine Rucker-Martin, Marianne Riou, Rui Adão, Boris Manoury, Mélanie Lambert, et al.

Circulation

ORIGINAL RESEARCH ARTICLE

Bmpr2 Mutant Rats Develop Pulmonary and Cardiac Characteristics of Pulmonary Arterial Hypertension

BACKGROUND: Monoallelic mutations in the gene encoding bone morphogenetic protein receptor 2 (*Bmpr2*) are the main genetic risk factor for heritable pulmonary arterial hypertension (PAH) with incomplete penetrance. Several *Bmpr2* transgenic mice have been reported to develop mild spontaneous PAH. In this study, we examined whether rats with the *Bmpr2* mutation were susceptible to developing more severe PAH.

METHODS: The zinc finger nuclease method was used to establish rat lines with mutations in the *Bmpr2* gene. These rats were then characterized at the hemodynamic, histological, electrophysiological, and molecular levels.

RESULTS: Rats with a monoallelic deletion of 71 bp in exon 1 (Δ*71* rats) showed decreased BMPRII expression and phosphorylated SMAD1/5/9 levels. Δ*71* Rats develop age-dependent spontaneous PAH with a low penetrance (16%–27%), similar to that in humans. Δ*71* Rats were more susceptible to hypoxia-induced pulmonary hypertension than wild-type rats. Δ*71* Rats exhibited progressive pulmonary vascular remodeling associated with a proproliferative phenotype and showed lower pulmonary microvascular density than wild-type rats. Organ bath studies revealed severe alteration of pulmonary artery contraction and relaxation associated with potassium channel subfamily K member 3 (KCNK3) dysfunction. High levels of perivascular fibrillar collagen and pulmonary interleukin-6 overexpression discriminated rats that developed spontaneous PAH and rats that did not develop spontaneous PAH. Finally, detailed assessments of cardiomyocytes demonstrated alterations in morphology, calcium (Ca^{2+}), and cell contractility specific to the right ventricle; these changes could explain the lower cardiac output of Δ*71* rats. Indeed, adult right ventricular cardiomyocytes from Δ*71* rats exhibited a smaller diameter, decreased sensitivity of sarcomeres to Ca^{2+}, decreased [Ca^{2+}] transient amplitude, reduced sarcoplasmic reticulum Ca^{2+} content, and short action potential duration compared with right ventricular cardiomyocytes from wild-type rats.

CONCLUSIONS: We characterized the first *Bmpr2* mutant rats and showed some of the critical cellular and molecular dysfunctions described in human PAH. We also identified the heart as an unexpected but potential target organ of *Bmpr2* mutations. Thus, this new genetic rat model represents a promising tool to study the pathogenesis of PAH.

Aurélie Hautefort, PhD
Pedro Mendes-Ferreira, PhD
Jessica Sabourin, PhD
Grégoire Manaud, MSc
Thomas Bertero, PhD
Catherine Rucker-Martin, PhD
Marianne Riou, MD
Rui Adão, PhD
Boris Manoury, PhD
Mélanie Lambert, MSc
Angèle Boet, MD
Florence Lecerf, MSc
Valérie Domergue, BS
Carmen Brás-Silva, PhD
Ana Maria Gomez, PhD
David Montani, MD, PhD
Barbara Girerd, PhD
Marc Humbert, MD, PhD
Fabrice Antigny, PhD*
Frédéric Perros, PhD*

*Drs Antigny and Perros contributed equally.

Key Words: bone morphogenetic protein receptors, type II ■ cardiovascular diseases ■ hypertension, pulmonary ■ interleukin-6 ■ models, animal ■ myocytes, cardiac

Sources of Funding, see page 946

https://www.ahajournals.org/journal/circ

Clinical Perspective

What Is New?

- We have created and characterized a new animal model of hereditary pulmonary arterial hypertension, which shares not only the same epidemiological characteristics with the human disease but also the same pathophysiological features observed in the pulmonary vasculature of patients with heritable pulmonary artery hypertension.
- Noticeably, we were able to show a not-yet-studied effect of bone morphogenetic protein receptor 2 (*Bmpr2*) mutation specifically on the right ventricle, which compromised intrinsic function, even in non-overloaded states.

What Are the Clinical Implications?

- The clinical implications for our findings are wide and show how *BMPR2* mutations compromise not only the pulmonary vasculature but also specifically the heart.
- Our data should result in an improved understanding of the intrinsic alterations of the right side of the heart in *BMPR2* mutation carriers, suggesting a deleterious effect of this mutation in right ventricular adaptation in carriers developing the disease and compromised response of these patients to standard therapy and lung transplantation.

Pulmonary arterial (PA) hypertension (PAH) is a severe, progressive disease clinically defined by an abnormal increase in pulmonary arterial pressure (PAP) >25 mm Hg and a PA wedge pressure of ≤15 mm Hg at rest, leading to right ventricular (RV) hypertrophy and ultimately death resulting from right heart failure.[1] Increased pulmonary vascular resistance responsible for PAH is the consequence of progressive reduction in the cross-sectional area of the lumen of distal PAs. In 70% of heritable PAH (hPAH) and 15% to 40% of idiopathic PAH (iPAH), the disease develops in the setting of germline autosomal dominant mutations in the bone morphogenetic protein receptor 2 (*BMPR2*) gene, making *BMPR2* mutations the main genetic risk factor for PAH development. However, the low penetrance (≈20%) of *BMPR2* mutations suggests that additional triggers are required for the development of PAH.[2] There is in particular an influence of sex on the development of PAH, with an approximate female:male ratio of 4:1, depending on the underlying disease pathology.[3] In the context of *BMPR2* mutation, this sexual dimorphism is also striking because the female penetrance of the mutations is ≈42% and the male penetrance is ≈14%.[4]

Bmpr2 transgenic mice display aberrant pulmonary vascular cell phenotypes, including excessive proliferation of medial smooth muscle cells (SMCs)[5] and apoptosis of endothelial cells (ECs). Johnson et al[6] demonstrated that *Bmpr2* mutations also induce endothelial disruption.

Rat models of pulmonary hypertension (PH) have undoubtedly contributed to a better understanding of the PH process. Rats are more sensitive to PH development than mice.[7] Moreover, recent developments of novel molecular tools such as transcription activator-like effector nucleases, zinc finger nuclease, and clustered regularly interspaced short palindromic repeats/Cas9 have enabled researchers to perform genome editing in rats.[8] We used these new technologies to establish a *Bmpr2* mutant rat model using the zinc finger nuclease method.

Accordingly, in this study, using a combination of hemodynamic measurements, molecular biology, electron microscopy, Ca^{2+} imaging, and electrophysiology approaches, we report the hemodynamic, histological, vascular, and molecular characterization of the first *Bmpr2* mutant rat line (harboring a monoallelic mutation) during aging.

METHODS

The *Bmpr2* mutant rat lines will be made available to other researchers for purposes of reproducing the results or replicating the procedure.

Generation of Bmpr2-Deficient Rats

Bmpr2 mutant rats were established using the zinc finger nuclease method (for details, see the online-only Data Supplement and Table I in the online-only Data Supplement).

The animal facility is licensed by the French Ministry of Agriculture (agreement C92-019-01). This study was approved by the Committee on the Ethics of Animal Experiments CEEA26 CAP Sud. Animal experiments were approved by the French Ministry of Higher Education. Animal experiments were performed conforming to the guidelines from Directive 2010/63/EU 22 (September 2010) of the European Parliament on the protection of animals used for scientific purposes and complied with French institution's guidelines for animal care and handling.

Bmpr2 Genotyping by Polymerase Chain Reaction

See the online-only Data Supplement.

Hemodynamic Measurements, Evaluation of RV Hypertrophy, and Collection of Tissues

See the online-only Data Supplement.

Histology and Immunohistochemistry
See the online-only Data Supplement.

Real-Time Quantitative Polymerase Chain Reaction
See the online-only Data Supplement.

Western Blot Analyses
See the online-only Data Supplement.

Isometric Tension Measurement
See the online-only Data Supplement.

Pulmonary Arterial SMC Isolation and Culture
See the online-only Data Supplement.

Adult Cardiomyocyte Isolation
See the online-only Data Supplement.

SMC Proliferation Assays
See the online-only Data Supplement.

Electrophysiological Recordings
See the online-only Data Supplement.

In Vitro Studies in Isolated Skinned Cardiomyocytes
See the online-only Data Supplement.

Measurement of $[Ca^{2+}]_i$ Transients and Sarcoplasmic Reticulum Ca^{2+} Load
See the online-only Data Supplement.

Transmission Electron Microscopy
See the online-only Data Supplement.

Correlative Light and Electron Microscopy
See the online-only Data Supplement.

Statistical Analysis
Analysis was performed with GraphPad Software version 6 (GraphPad Software Inc, San Diego, CA). All data were verified for normal distributions. Quantitative variables are presented as mean± SEM. Data were analyzed with Student *t* tests or 1-way ANOVA and Bonferroni multiple-comparisons tests. For the isolated cardiomyocyte experiments, 2-way ANOVA with repeated measures was used to analyze most parameters with the Tukey method for post hoc comparisons between groups. The Student *t* test was used for calcium half-maximal effective concentration. Values of $P<0.05$ were considered statistically significant.

RESULTS

Monoallelic Bmpr2 Mutations in Rats Reduced the BMPRII Canonical Signaling Pathway in the Lungs
Zinc finger nuclease technology targeting the first exon of the *Bmpr2* gene induced a monoallelic deletion of 71 bp (Δ*71*), which led to loss of an initiation codon (Figure 1A and 1B). In this study, we focused only on males because hemodynamic and histological alterations were observed in males but not in females (Figure I in the online-only Data Supplement). Females nevertheless had a similar level of pulmonary BMPRII expression (data not shown). We performed Western blot analysis to evaluate the effects of monoallelic *Bmpr2* mutations on pulmonary BMPRII protein expression and canonical BMPRII signaling pathways. As expected, we observed a 50% decrease in the expression of BMPRII in the lungs of *Bmpr2* mutant rats (Figure 1C), validating our strategy. Because BMPRII signaling involves the SMAD pathway, we also showed a significant decrease in the phosphorylation of SMAD1/5/9 in the lungs of Δ*71* rats (Figure 1C). Similar results were obtained in the second *Bmpr2* mutant rat line (Δ*140* rats; Figure IIA through IIC in the online-only Data Supplement). When we mated rats with monoallelic *Bmpr2* mutations, we did not obtain biallelic mutation–bearing rats, and we observed a significant decrease in the number of pups (data not shown). This suggested that biallelic *Bmpr2* mutations were lethal in utero, consistent with a previous study demonstrating that homozygosity for a null mutation in *Bmpr2* is lethal before gastrulation.[9]

Bmpr2 Mutant Rats Developed Spontaneous PH in an Age-Dependent Manner Concomitant With Alterations in Distal Microvascular Density
We performed right-sided heart catheterization in wild-type (WT) and Δ*71* rats at 3, 6, and 12 months of age. Spontaneous PH (SPH) was defined by an mean PA pressure ≥25 mm Hg. As shown in Figure 2A, no SPH was observed in Δ*71* rats at 3 months of age, as observed by RV hypertrophy (Fulton index), cardiac output (CO), total pulmonary vascular resistance (Figure 2A), and carotid artery systemic pressure (data not shown) results similar to those of WT rats. However, 16.7% of animals (5 of 30) had SPH at 6 months of age in association with a significant increase in total pulmonary vascular resistance (Figure 2B). All Δ*71* rats exhibited a significant decrease in CO (Figure 2B). At

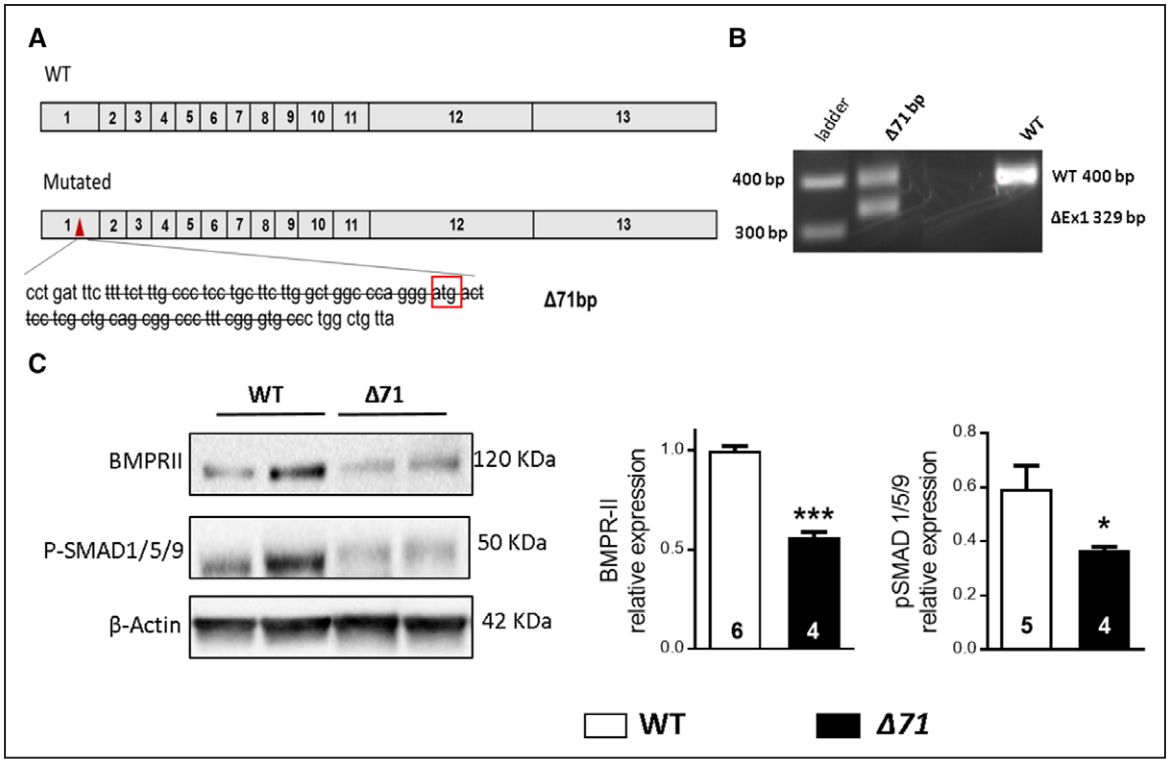

Figure 1. Generation and characterization of heterozygous bone morphogenetic protein receptor 2 (*Bmpr2*) mutant rats.
A, Schematic overview of the *Bmpr2* gene with wild-type (WT) and *Bmpr2* mutant alleles. We generated *Bmpr2* mutant rats with a monoallelic deletion of 71 bp (Δ*71*) in exon 1 of the *Bmpr2* gene, inducing the loss of the start codon (box). **B**, Validation of deletions by polymerase chain reaction, showing genomic DNA amplicons from rats carrying the WT and deleted alleles. Primers targeting the edges of deleted sequences detecting the WT allele (WT, 400 bp) and the allele with the deletion (Δ*Ex1*, 329 bp). **C**, Representative Western blots and quantification of BMPR-II expression and phospho-SMAD1/5/9 levels in lungs from WT (n=5; white) and Δ*71* (n=4; black) rats. β-Actin was used as loading control. Results are presented as mean±SEM. ns indicates not significant. **P*<0.05; ****P*<0.001.

1 year, the penetrance of SPH was increased up to 27.8% (10 of 36), with concomitant increases in mean PA pressure, total pulmonary vascular resistance, and RV hypertrophy and a decrease in CO (Figure 2C). CO was also lower in non-SPH rats (Figure 2C). The second *Bmpr2* mutant rat line (Δ*140* rats) developed SPH at 12 months of age with a penetrance of 20% (5 of 25; Figure IIF in the online-only Data Supplement). Although Δ*71* females did not develop SPH, their CO values tended to be lower at 6 months of age and were significantly lower at 12 months of age (Figure I in the online-only Data Supplement). The lower CO found in mutant rats may nevertheless be related at least in part to lower body weight (Tables II and III in the online-only Data Supplement). However, there is a complex interplay between the bone morphogenetic protein signaling and body development,[10,11] and *Bmpr2* mutations may be responsible for weight and height abnormalities.

In WT rats, the density of pulmonary small microvessels (<10 μm), expressed as number of $CD31^+$ vessels measured in 20 fields, progressively increased over time (23.4±4.7, 30.0±6.1, and 42.1±5.1 at 3, 6, and 12 months, respectively), whereas the density of larger microvessels (between 10 and 50 μm) remained constant (44.0±5.8, 31.0±2.7, and 36.0±3.9, respectively) in WT rats (Figure 2D through 2G). Conversely, the density of pulmonary small microvessels (<10 μm) did not increase over time in Δ*71* rats (18.0±2.8, 17.0±2.7, and 24.0±3 at 3, 6, and 12 months, respectively). Consequently, compared with that in WT rats, the density of pulmonary small microvessels became significantly lower at 6 months of age (*P*<0.05) and even lower at 12 months of age (*P*<0.01; Figure 2D–2G).

Bmpr2 Mutant Rats With SPH Exhibited Interleukin-6 Overexpression

In an attempt to identify a molecular marker of disease penetrance, we quantified the expression of the proinflammatory cytokine interleukin (IL)-6 in lungs from affected and unaffected animals compared with controls. Indeed, patients with iPAH exhibit increased IL-6 serum levels, which correlate with their prognoses.[12] Consistent with these findings, lung-specific IL-6 transgenic mice display SPH in normoxia and develop greatly exaggerated hypoxia-induced PH,[13] whereas IL-6 receptor–deficient mice show resistance to hypoxia-induced PH.[14] These findings suggest that IL-6 has a significant role in the pathogenesis of PH. Consistent with these observations, IL-6 was specifically overexpressed in *Bmpr2* mutant rats with SPH, whereas non-SPH rats had levels similar to those of controls (Figure III in the online-only Data Supplement).

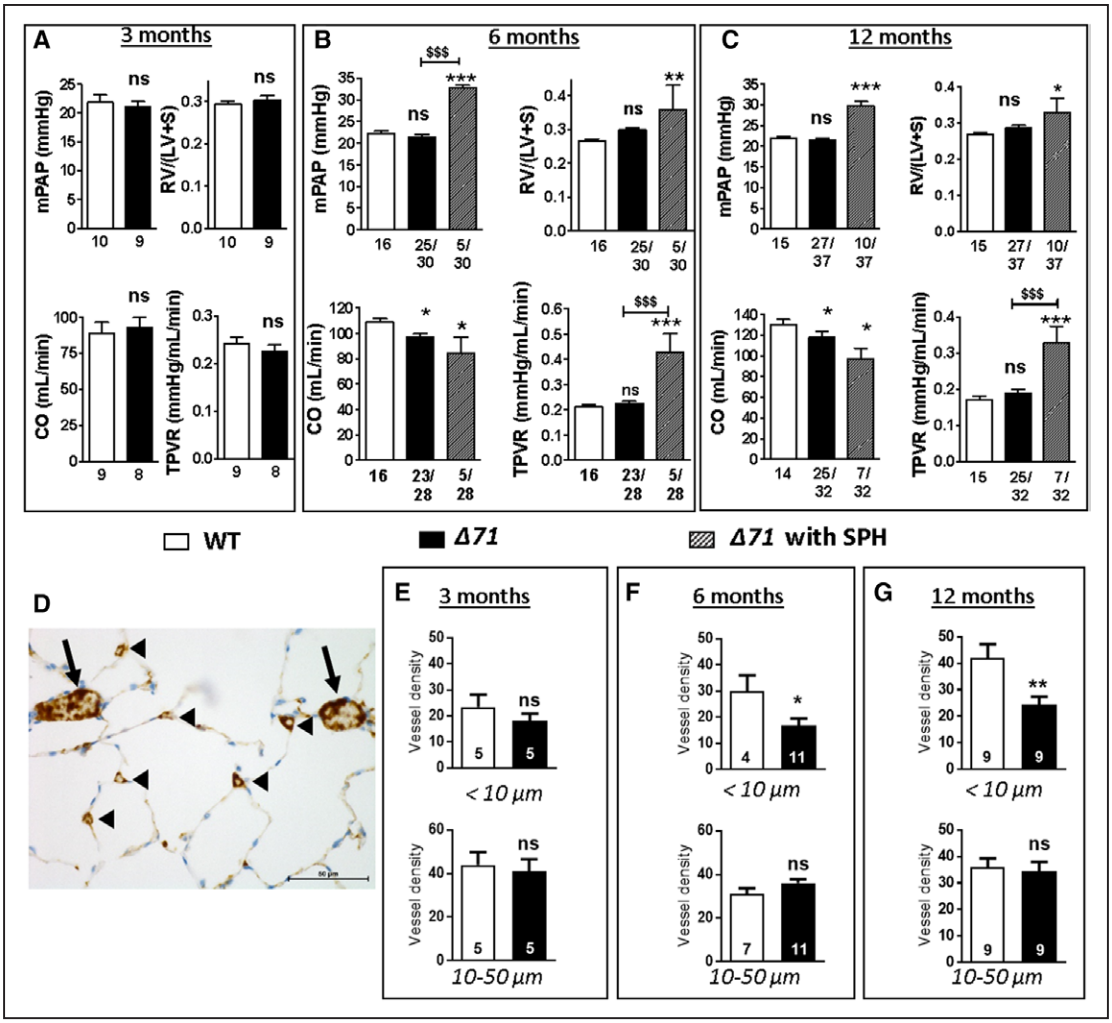

Figure 2. Bone morphogenetic protein receptor 2 (*Bmpr2*) mutant rats developed spontaneous pulmonary hypertension (SPH) in an age-dependent manner concomitant with alterations in distal microvascular density.

Assessment of mean pulmonary artery pressure (mPAP), cardiac output (CO), total pulmonary vascular resistance (TPVR), right ventricular hypertrophy (Fulton index; weight ratio of right ventricle [RV] to left ventricle [LV] plus septum [S]) in Δ*71* male rats without SPH (black) and wild-type (WT) male rats (white) at 3 (**A**), 6 (**B**), and 12 (**C**) months of age. *Bmpr2* mutant rats were thought to have SPH when the mPAP was ≥25 mm Hg. SPH Δ*71* rats are indicated with black-striped bars. **D** through **G**, Pulmonary vessel density quantification based on CD31 (endothelium marker) labeling of paraffin-embedded lung sections, expressed as number of $CD31^+$ vessels measured in 20 fields (**D**; vessel diameter >10 µm, arrows; vessel diameter <10 µm, arrowheads) from Δ*71* without SPH (black) compared with WT (white) rats at 3 (**E**), 6 (**F**), and 12 (**G**) months of age. Vessel diameter <10 µm (**top**) and vessel diameter >10 µm (**bottom**). Each group at each time point includes different animals. ns indicates not significant. **P*<0.05, ***P*<0.01, ****P*<0.001 vs WT. $$$*P*<0.001 vs rats without SPH.

Bmpr2 Mutant Rats Were More Susceptible to Chronic Hypoxia-Induced PH

To investigate whether *Bmpr2* mutations sensitized rats to chronic hypoxia-induced PH, we exposed 3-month-old Δ*71* rats to 10% O_2 for 3 weeks. *Bmpr2* mutations increased the severity of hypoxic PH, as demonstrated by the observation that Δ*71* rats had higher mean PA pressure values compared with WT rats at the end of the experiment (Figure IV in the online-only Data Supplement).

Bmpr2 Mutations Increased the Muscularization of the Distal Pulmonary Vascular Bed

Δ*71* Rats had higher muscularization of smaller vessels (diameter <50 µm) at all analyzed time points (3, 6, and 12 months of age) compared with WT rats (Figure 3A through 3D). Muscularization of larger vessels with diameters of 50 to 100 µm became significantly higher only at the latest time point (12 months of age; Figure 3A through 3D). We obtained similar results in the Δ*140* strain (Figure IIG through III in the online-only Data Supplement). Moreover, Western blotting of the proproliferative mitogen-activated protein kinase pathway in lung tissues from Δ*71* rats revealed that the phosphorylation of p38 mitogen-activated protein kinase was increased compared with that in WT rats at 1 year of age (Figure 3E). In addition, extracellular signal–regulated kinase 1/2 phosphorylation was significantly higher than in WT rats at earlier time points (3 and 6 months of age; Figure 3F). In vitro, PASMCs isolated from 6-month-old Δ*71* rats had higher proliferation rates than those isolated from WT rats after treatment

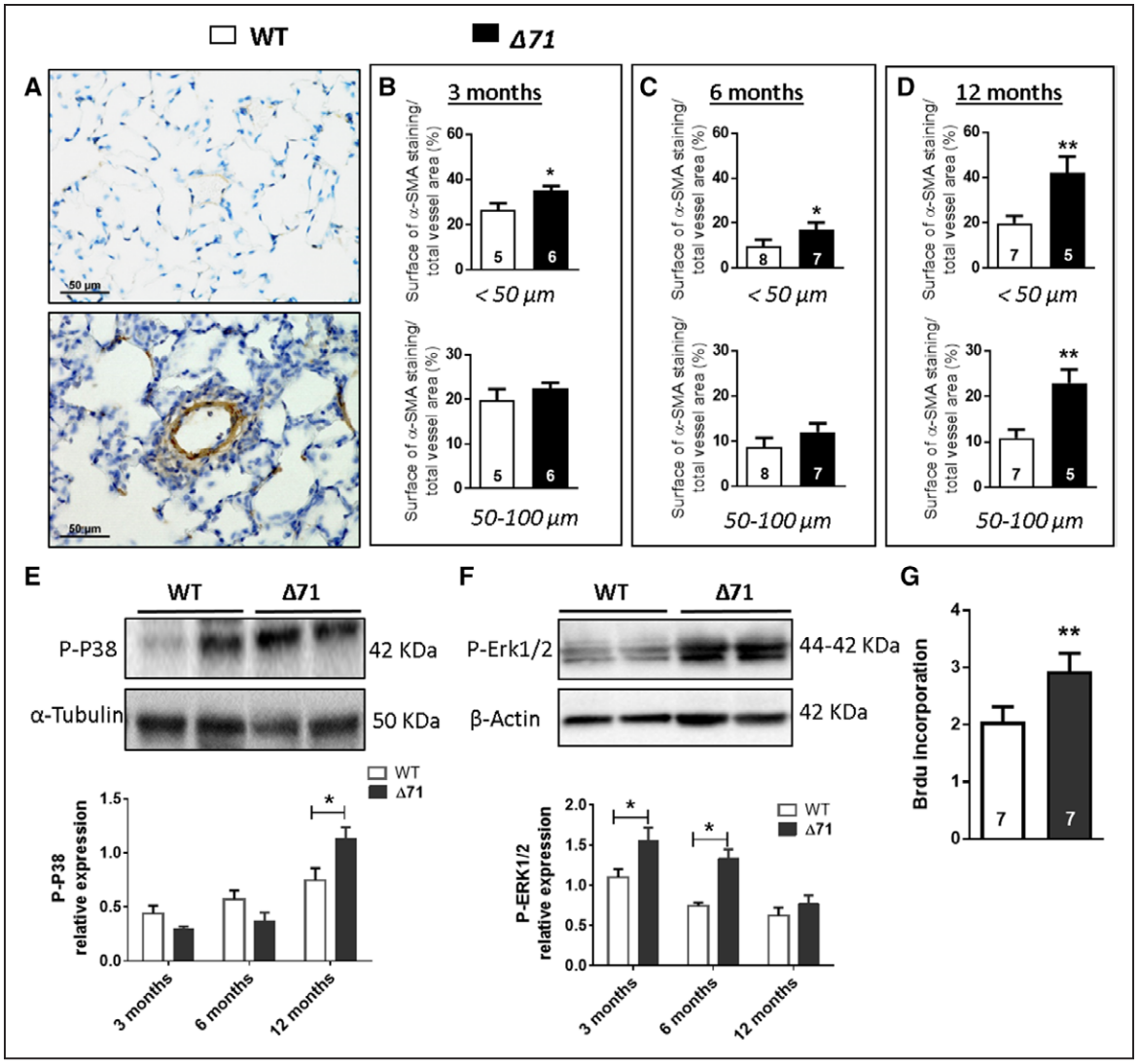

Figure 3. Bone morphogenetic protein receptor 2 (*Bmpr2*) mutations increased the muscularization of the distal pulmonary vascular bed and enhanced pulmonary artery smooth muscle cell (PASMC) proliferation.

A through **D**, Vessel muscularization analysis based on α-actin smooth muscle labeling on paraffin-embedded lung sections (**A**; **top**, wild-type [WT]; **bottom**, Δ*71*) from Δ*71* (black) without spontaneous pulmonary hypertension (SPH) and WT (white) rats at 3 (**B**), 6 (**C**), and 12 (**D**) months of age. Vessel diameter <50 µm (**top**) and vessel diameter between 50 and 100 µm (**bottom**). **E** and **F**, Western blotting of (**E**) p38 phosphorylation (p) at 12 months of age and (**F**) extracellular signal–regulated kinase (ERK) 1/2 phosphorylation at 6 months of age in the lungs of Δ*71* (black) rats without SPH and WT (white) rats and quantification of (**E**) p38 and (**F**) ERK1/2 phosphorylation levels in the lung of Δ*71* (black) without SPH and WT (white) rats at 3, 6, and 12 months of age. β-Actin and α-tubulin were used as loading controls. **G**, Proliferation was measured with BrdU incorporation. Proliferation of PASMCs from Δ*71* without SPH (black) and WT (white) rats after 24 hours of starvation, followed by treatment with platelet-derived growth factor-BB (10 ng/mL) for 24 hours (n=7 for each group). ns indicates not significant. **P*<0.05; ***P*<0.01.

with platelet-derived growth factor-BB (10 ng/mL) for 24 hours (Figure 3G).

Bmpr2 Deficiency Increased Perivascular Fibrillar Collagen Deposition and Assembly in Distal Pulmonary Arteries

Perivascular fibrillar collagen deposition and assembly were analyzed in Δ*71* rats (Figure 4 and Figure V in the online-only Data Supplement). Although increased perivascular collagen deposition was observed in both small (<50 µm; Figure 4) and medium (50–100 µm; Figure V in the online-only Data Supplement) PAs from Δ*71* rats at 3, 6, and 12 months of age compared with WT rats, a significantly higher level of fibrillar collagen assembly was also observed in both small and medium PAs in Δ*71* rats with SPH at 6 and 12 months of age compared with Δ*71* rats without SPH at 6 and 12 months of age.

Bmpr2 Mutations Induced Lung Inflammation During Aging

We analyzed the effects of *Bmpr2* deficiency in pulmonary inflammation by quantifying the expression of pulmonary CD45 protein (a pan leukocyte marker). We

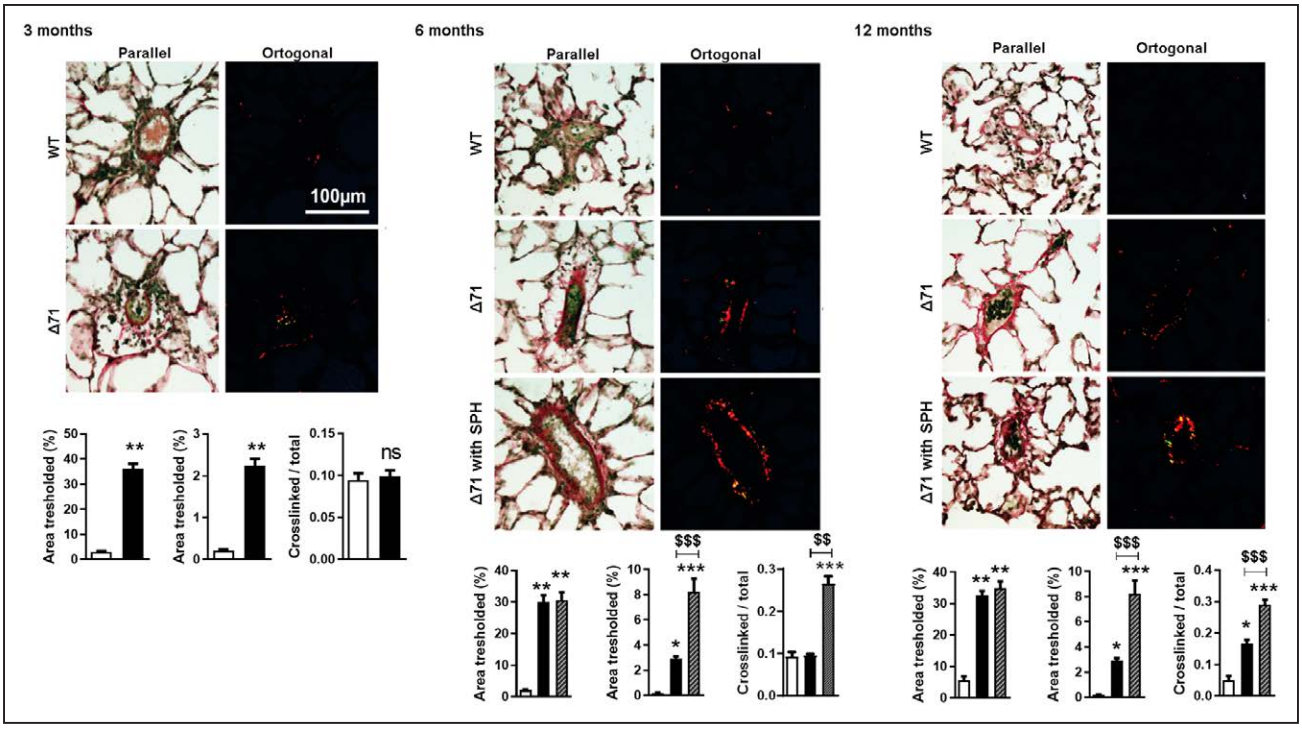

Figure 4. Bone morphogenetic protein receptor 2 (*Bmpr2*) mutations increased perivascular fibrillar collagen deposition and assembly in distal (diameters <50 µm) pulmonary arteries.

Picrosirius Red staining and quantification of orthogonal signals in pulmonary arteries (diameters <50 µm) from *Δ71* rats with (black-striped bars) or without (black) spontaneous pulmonary hypertension (SPH) vs wild-type (WT; white) rats at 3, 6, and 12 months of age (n=5 for each group). Scale bar, 100 µm. **P*<0.05, ***P*<0.01, ****P*<0.001 vs WT. $$*P*<0.01 and $$$*P*<0.001 vs rats without SPH.

showed that lung CD45 expression was significantly increased in Δ*71* rats at 1 year of age compared with WT rats (Figure VIA in the online-only Data Supplement). Hematoxylin-eosin staining revealed perivascular leukocyte accumulation at this later time point (Figure VIB in the online-only Data Supplement).

Bmpr2 Deficiency Caused Abnormal PA Contraction, PASMC Depolarization, Alteration of KCNK3 Function, and Reduced Endothelium-Dependent PA Relaxation

We induced contraction of PAs isolated from 6-month-old WT and Δ*71* rats by increasing the KCl concentration (from 10–120 mmol/L) to progressively depolarize PASMCs (Figure 5A). The contractile dose-response to KCl was significantly shifted to the left in PAs from Δ*71* rats, demonstrating a predisposition to contraction (Figure 5A). We also studied endothelium-dependent PA relaxation from WT and Δ*71* rats by evaluating the dose response to acetylcholine after precontraction of PA with the thromboxane A_2 agonist U46619 (1 µmol/L). PAs from Δ*71* rats exhibited a significant decrease in acetylcholine-induced relaxation compared with WT rats (at 10 µmol/L acetylcholine; Figure 5B). This functional alteration occurred with ultrastructural changes in ECs. Indeed, electron microscopy imaging of remodeled PAs from Δ*71* rats demonstrated disjointed and protrusive ECs containing abnormal vacuoles (Figure VII in the online-only Data Supplement).

Because the membrane potential (Em) of PASMCs partly controls the tone of PAs,[15] we used a whole-cell patch-clamp technique in current-clamp mode to measure resting Em in freshly isolated PASMCs from Δ*71* and WT rats. We observed a significant depolarization of the Em in Δ*71* rats (Figure 5C). To explain this cellular depolarization, we analyzed the KCNK3 current (I_{KNCK3}), which strongly contributes to resting Em of PAMSCs.[15] Using the specific KCNK3 inhibitor A293 (200 nmol/L), we isolated the KCNK3 current from all K^+ currents (A293-sensitive current). The A293-sensitive current (I_{KCNK3}) was strongly reduced in freshly isolated PASMCs from Δ*71* rats (Figure 5D). KCNK3 channels are known to be insensitive to Tetraethylammonium inhibited by external acidic pH (pH 6.3), and fully activated at basic pH (8.3). In another protocol, we evaluated the KCNK3 current through measurement of the Tetraethylammonium-insensitive acidic-sensitive K^+ current.[15] This current was also reduced in PASMCs from Δ*71* rats, confirming that KCNK3 function was strongly reduced in the context of *Bmpr2* mutations (Figure 5E). However, KCNK3 expression was not affected at the mRNA level in Δ*71* rats (Figure 5F).

To explain the loss of KCNK3 function, we hypothesized that KCNK3 was not correctly localized to the plasma membrane. Accordingly, we analyzed the sub-

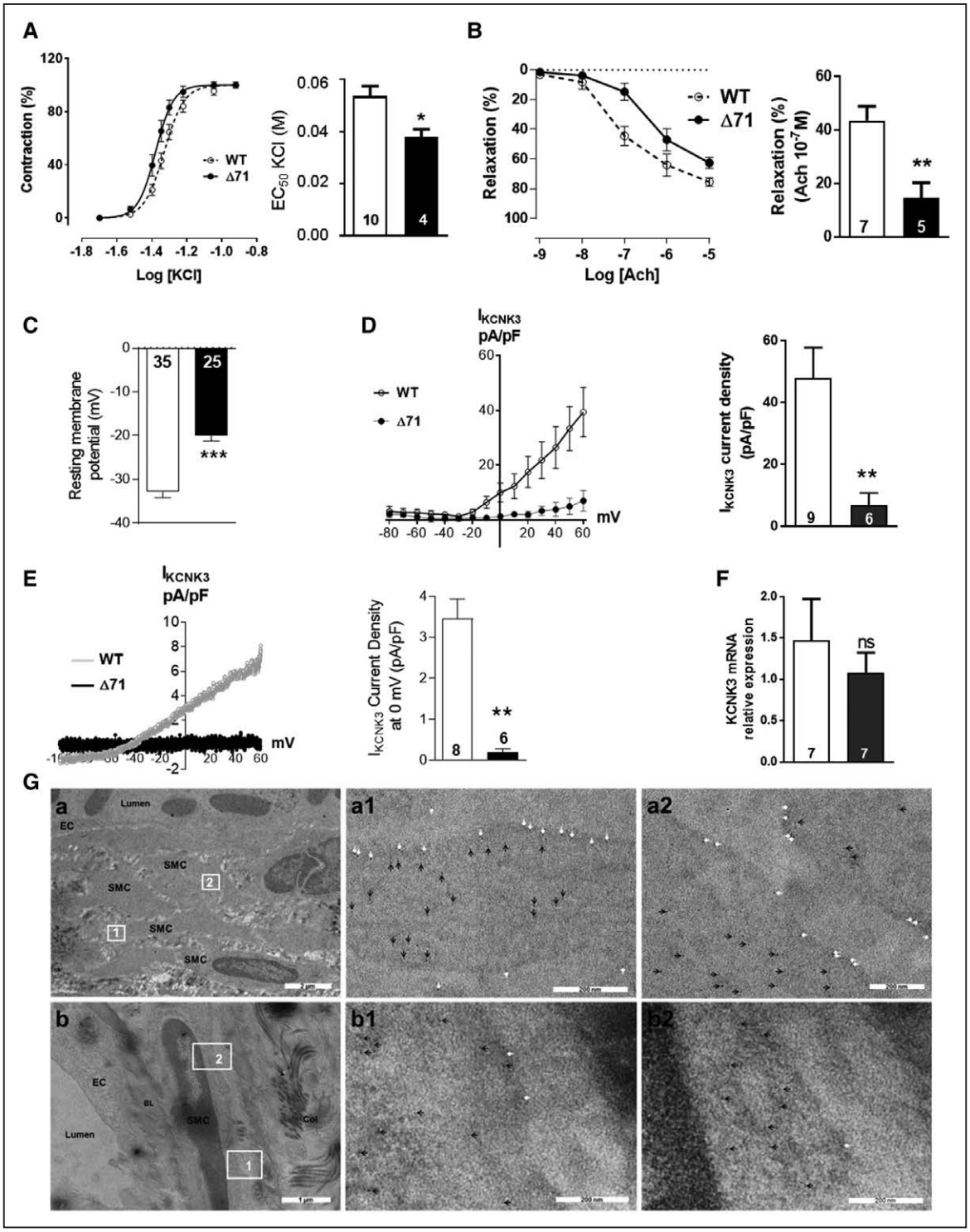

Figure 5. Bone morphogenetic protein receptor 2 (*Bmpr2*) deficiency led to abnormal pulmonary artery (PA) contraction, PA smooth muscle cell (SMC) plasma membrane depolarization, altered potassium channel subfamily K member 3 (KCNK3) function, and endothelium-dependent PA relaxation. **A**, **Left**, Dose-response curve established by applying increasing concentrations of KCl (10–120 mmol/L) in PAs isolated from Δ*71* (n=4; black curve) and wild-type (WT; n=10; white curve) rats. **Right**, Half-maximal effective concentration (EC_{50}) of KCl under previous conditions. **B**, **Left**, Relaxation dose-response curves established by applying increasing concentrations of acetylcholine (Ach; 1 nmol/L to 10 μmol/L) on PA segments isolated from Δ*71* (n=5; black) and WT (n=7; white) rats. **Right**, Corresponding bar graph of the percent relaxation at 10^{-7} mol/L of Ach. **C**, Resting membrane potential (Em) of PASMCs that were freshly isolated from Δ*71* (black) or WT (white, Em; 3 rats per condition; 25<n<35 cells). **D**, Current-voltage relationships of A293–K^+-sensitive current (I_{KCNK3}) in PASMCs freshly isolated from Δ*71* (n=6–10; black) and WT (n=9–14; white) rats. Bar graph represents KCNK3 current density measured at 60 mV for each condition. **E**, **Left**, Representative ramp currents in freshly isolated PASMCs from WT and Δ*71* rats, corresponding to the differences between the currents recorded at pH 8.3 and 6.3, called the acidic-sensitive K^+ current. **Right**, Quantification of KCNK3 current density measured at 0 mV (6 <n <7 cells). **F**, mRNA expression of *KCNK3* in PAs from Δ*71* and WT rats (n=7 rats). **G**, Transmission electron microscopy of pulmonary arteries from (**a**) WT and (**b**) Δ*71* without spontaneous pulmonary hypertension (SPH) rats after KCNK3 staining. White squares correspond to ×2 magnification of SMCs 1 and 2. White arrows indicate plasma membrane KCNK3 localization; black arrows, cytoplasmic KCNK3 localization. BL indicates basal lamina; Col, collagen; EC, endothelial cell; E, elastic; F, fibroblast; N, nucleus; and ns, not significant, **P*<0.05; ***P*<0.01; ****P*<0.001.

cellular localization of KCNK3 using correlative light and electron microscopy. As shown in Figure 5G, KCNK3 was expressed mainly at the cell surface of PASMCs from WT rats, whereas KCNK3 was not present at the cell surface of PASMCs from Δ*71* rats and was abnormally retained in the cytosol and sarcoplasmic reticulum (SR) compartments.

Bmpr2 Mutant Rats Showed Intrinsic RV Dysfunction

Hemodynamic measurements revealed a decrease in cardiac output in all Δ*71* rats at 6 and 12 months of age (Figure 2), suggesting abnormalities in cardiac function in those animals. Using frozen RV and left ventricular (LV) samples from Δ*71* rats without SPH at 6 months of age, we next measured the active tension of isolated cardiomyocytes. As shown in Figure 6, isolated skinned cardiomyocytes in RV samples from Δ*71* rats showed a significant decrease in active tension development (Figure 6A) and a decreased sensitivity to calcium ($P<0.05$; Figure 6B and 6C), whereas no changes were observed in passive tension (Figure 6D). Notably, no significant modifications were detected in LV cardiomyocytes (Figure 6E through 6H). The intrinsic RV dysfunction occurring in unaffected Δ*71* rats was not associated with decreased RV capillarization or RV fibrosis (Figure VIIIA and VIIIB in the online-only Data Supplement).

Bmpr2 Mutant RV Cardiomyocytes Showed Decreased $[Ca^{2+}]_i$ Transients, SR Ca^{2+} Load, and Cell Shortening

Decreased CO could also be related to alterations in Ca^{2+} handling involved in excitation-contraction coupling. We analyzed electrically evoked $[Ca^{2+}]_i$ transients and cell shortening in isolated RV and LV cardiomyocytes from WT and Δ*71* rats without SPH (6 months of age). Figure 7A shows representative line-scan images (top) and corresponding fluorescence traces (bottom) of Fluo-4–loaded RV cardiomyocytes from WT and Δ*71* rats on field stimulation at 1 Hz. The $[Ca^{2+}]_i$ transient amplitude was significantly decreased in RV cardiomyocytes from Δ*71* rats (Figure 7A and 7B), demonstrating compromised Ca^{2+} handling. The $[Ca^{2+}]_i$ transient decay time was unchanged (Figure 7C), suggesting similar Ca^{2+} uptake by the SR calcium transport ATPase pump in WT and *Bmpr2*-deficient rats. Consistent with this, we found no significant changes in SR Ca^{2+}-ATPase expression, total phospholamban expression, or phospholamban phosphorylation at serine 16/threonine 17 (Figure 7E). The decrease in the amplitude of $[Ca^{2+}]_i$ transients was associated with a decrease in cell shortening in RV myocytes from Δ*71* rats (Figure 7D). No significant modifications were detected in LV cardiomyocytes (Figure IXA through IXC in the online-only Data Supplement).

SR Ca^{2+} content is a determinant of the $[Ca^{2+}]_i$ transient peak amplitude; therefore, we estimated SR Ca^{2+} loading by rapid caffeine application (10 mmol/L), as exemplified in Figure 7F for RV cardiomyocytes from WT and Δ*71* rats. Caffeine-evoked $[Ca^{2+}]_i$ transients in RV myocytes were significantly reduced in *Bmpr2*-deficient cardiomyocytes compared with WT cardiomyocytes (Figure 7F and 7G). Thus, the decrease in the amplitude of $[Ca^{2+}]_i$ transients may be related, at least in part, to the reduction in SR Ca^{2+} load. The decay time of caffeine-induced $[Ca^{2+}]_i$ transients was similar in myocytes from WT and Δ*71* rats (Figure 7H), suggesting that Na^+/Ca^{2+} exchange activity was maintained. We also estimated the fractional release in electrically evoked twitches by normalizing the $[Ca^{2+}]_i$ transient amplitude to the SR Ca^{2+} load. We showed similar fractional release in isolated cardiomyocytes from Δ*71* rats and WT cardiomyocytes (Figure 7I), suggesting unchanged Ca^{2+}-induced Ca^{2+}-released efficiency. No significant modifications were detected in LV cardiomyocytes (Figure IXA through IXE in the online-only Data Supplement).

Bmpr2 Deficiency Was Associated With Decreased RV Cardiomyocyte Size and Action Potential Remodeling

Reduction of SR Ca^{2+} content and $[Ca^{2+}]_i$ transients is traditionally observed in left-sided heart hypertrophy and failure,[16] which is associated with electrophysiological remodeling, including action potential prolongation and decreased outward K^+ current.[16] Using the whole-cell patch-clamp approach, we evaluated the cell surface of isolated RV cardiomyocytes from WT and Δ*71* rats (at 6 months of age) by measuring the cell capacitance. The cell capacitance of cardiomyocytes isolated from Δ*71* rats was significantly reduced compared with those from WT rats, indicating a decrease in the cell surface area (Figure 8A). By measuring the diameters of RV cardiomyocytes in histological sections, we confirmed that the diameter of RV cardiomyocytes was decreased in Δ*71* rats compared with WT rats (Figure 8B), whereas cardiomyocyte size was unchanged in the LV compartment (data not shown).

To determine the effects of *Bmpr2* deficiency on RV action potential, we analyzed action potential duration by patch-clamp experiments. We demonstrated that action potential repolarization was significantly shortened at –30 mV in RV cardiomyocytes from Δ*71* rats compared with WT rats (Figure 8C and 8D). Transient (I_{to}) and sustained (I_{sus}) outward K^+ currents play a critical role in action potential repolarization. Thus, we analyzed I_{to} and I_{sus} in RV cardiomyocytes from Δ*71* rats. The results indicated that I_{to} was significantly increased in Δ*71* rats,

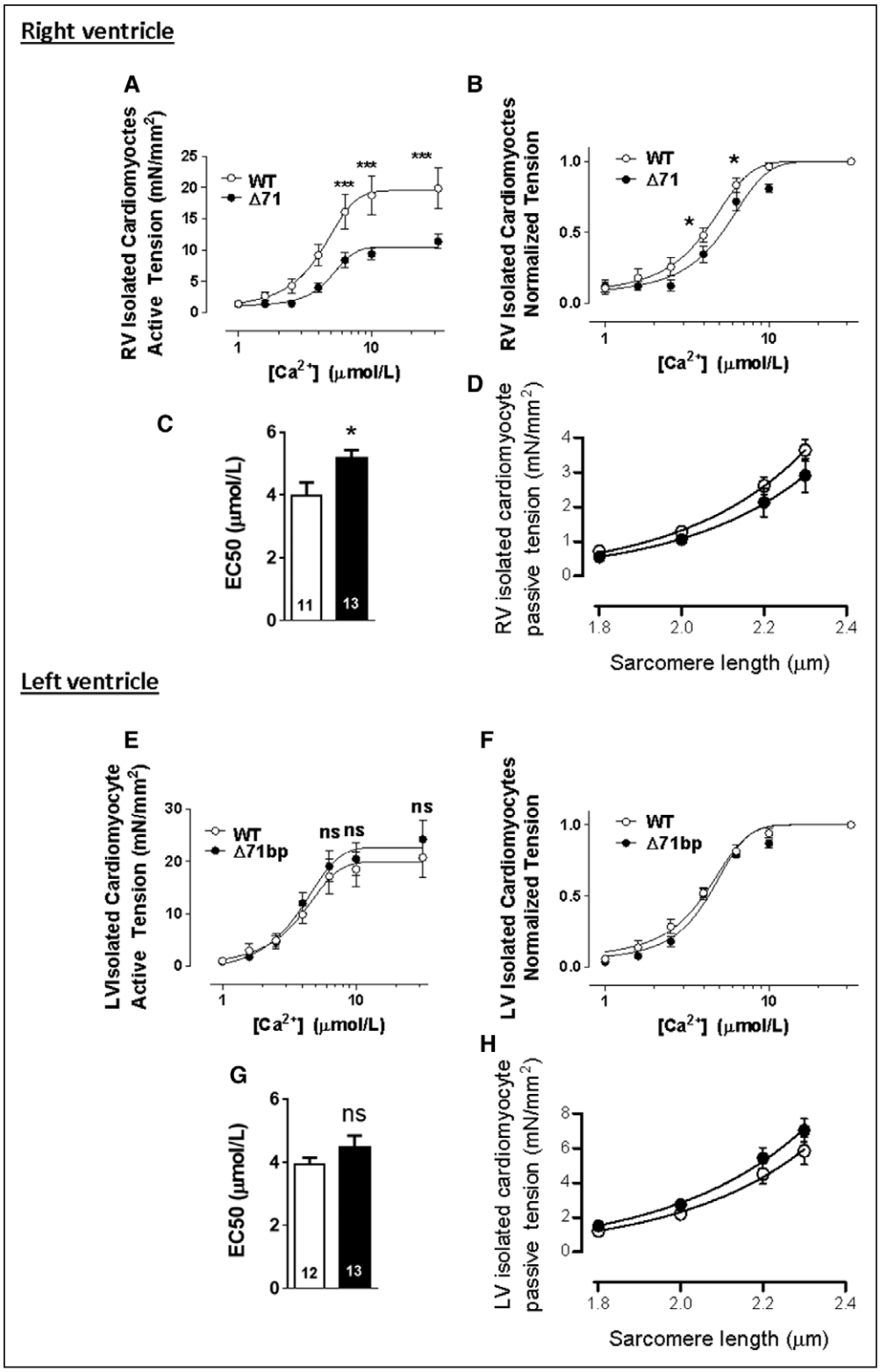

Figure 6. Isolated skinned cardiomyocytes specifically from the right ventricle (RV) of bone morphogenetic protein receptor 2 (*Bmpr2*)–deficient rats showed decreased active tension development and decreased sensitivity to calcium at 6 months of age.
In the RV compartment (**A**), the active tension–Ca^{2+} curve showed a significant decrease in tension development in cardiomyocytes isolated from Δ*71* rats without spontaneous pulmonary hypertension (SPH) compared with those isolated from wild-type (WT) rats. **B**, The normalized tension–Ca^{2+} curve showed a rightward shift in Δ*71* rats without SPH compared with WT rats. **C**, Calcium sensitivity was decreased in Δ*71* rats without SPH compared with WT rats. EC_{50} for Ca^{2+} is the Ca^{2+} concentration at which 50% of tension was developed. **D**, The passive tension–sarcomere length curve showed no differences between Δ*71* rats without SPH and WT rats. In the left ventricular (LV) compartment (**E**), the active tension–Ca^{2+} curve, (**F**) normalized tension–Ca^{2+} curve, (**G**) EC_{50}, and (**H**) passive tension–sarcomere length curve. ns indicates not significant were not changed between groups. **P*<0.05; ****P*<0.001.

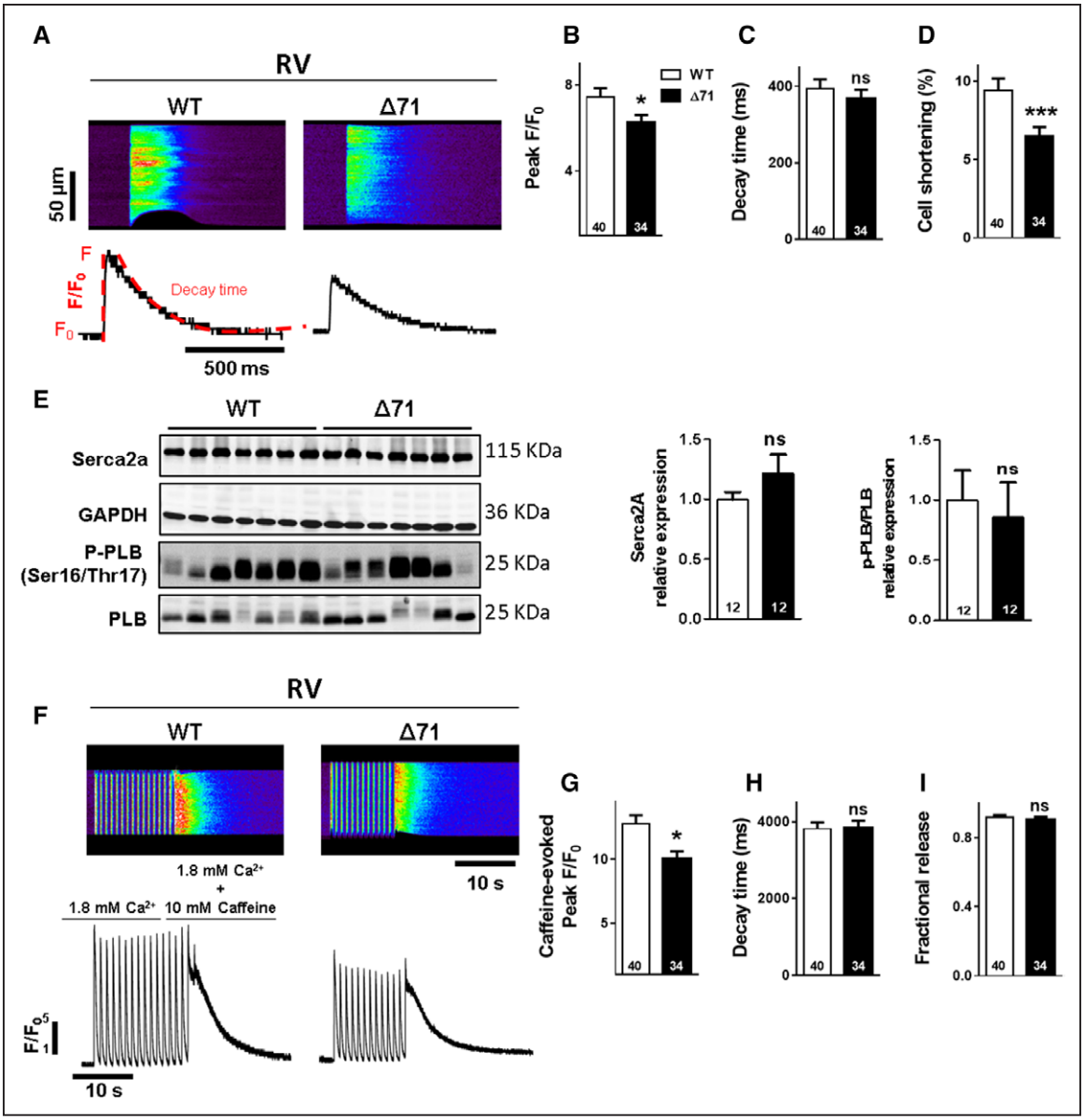

Figure 7. Decreased $[Ca^{2+}]_i$ transients, sarcoplasmic reticulum (SR) Ca^{2+} load, and cell shortening in right ventricular (RV) cardiomyocytes from bone morphogenetic protein receptor 2 (*Bmpr2*)–deficient rats at 6 months of age.

A, **Top**, Line scan of isolated RV cardiomyocytes loaded with Fluo-4/AM from Δ*71* and wild-type (WT) rats. **Bottom**, Corresponding traces of $[Ca^{2+}]_i$ transients. **B**, Amplitude of $[Ca^{2+}]_i$ transients (peak F/F_0) obtained in RV myocytes field-stimulated at 1 Hz in Δ*71* and WT rats. **C**, Average of $[Ca^{2+}]_i$ transients decay time (milliseconds) in RV myocytes in WT and Δ*71* rats. **D**, Average percent cell shortening in RV myocytes in Δ*71* and WT rats. **E**, **Left**, Representative Western blots of SR Ca2+-ATPase (SERCA2a), phospho-serine 16 (Ser17) / phospho-threonine 17 phospholamban (PLB), and total PLB levels in RV tissue from Δ*71* and WT rats. GAPDH was used as a loading control. **Middle** and **Right**, Quantification of SERCA2a expression and the phospho-PLB/PLB ratio (n=12 different rats). **F**, Evaluation of SR Ca^{2+} load in single RV cardiomyocytes from Δ*71* and WT rats. **Top**, Line scan of isolated RV cardiomyocytes loaded with Fluo-4/AM from WT and Δ*71* rats. **Bottom**, Corresponding traces of caffeine-induced $[Ca^{2+}]_i$ transients. **G**, Amplitude of caffeine-induced SR Ca^{2+} load (peak F/F_0) recorded in RV myocytes from Δ*71* and WT rats. **H**, Average of caffeine-evoked SR Ca^{2+} load decay time in RV myocytes from Δ*71* and WT rats. **I**, Average fractional release in RV myocytes from Δ*71* and WT rats. ns indicates not significant. **P*<0.05; ****P*<0.001.

whereas I_{sus} was unchanged (Figure 8E and 8F), similar to I_{K1} (Figure IXF in the online-only Data Supplement), suggesting a key role of I_{to} in action potential shortening.

DISCUSSION

In this study, we performed hemodynamic, histological, cellular, electrophysiological, and molecular characterization of 2 *Bmpr2*-deficient rat lines (Δ*71* and Δ*140*). This study has 5 major findings, as follows. First, we succeeded in generating a model of *Bmpr2* haploinsufficiency with a 50% decrease in BMPRII lung expression associated with reduced activation of SMAD1/5/9 downstream signaling. Second, *Bmpr2*-deficient rats developed SPH in an age-dependent manner with a penetrance ranging between 16.7% and 27.8%, perfectly mimicking the PAH penetrance in patients carrying a *BMPR2* mutation, and were more susceptible to chronic

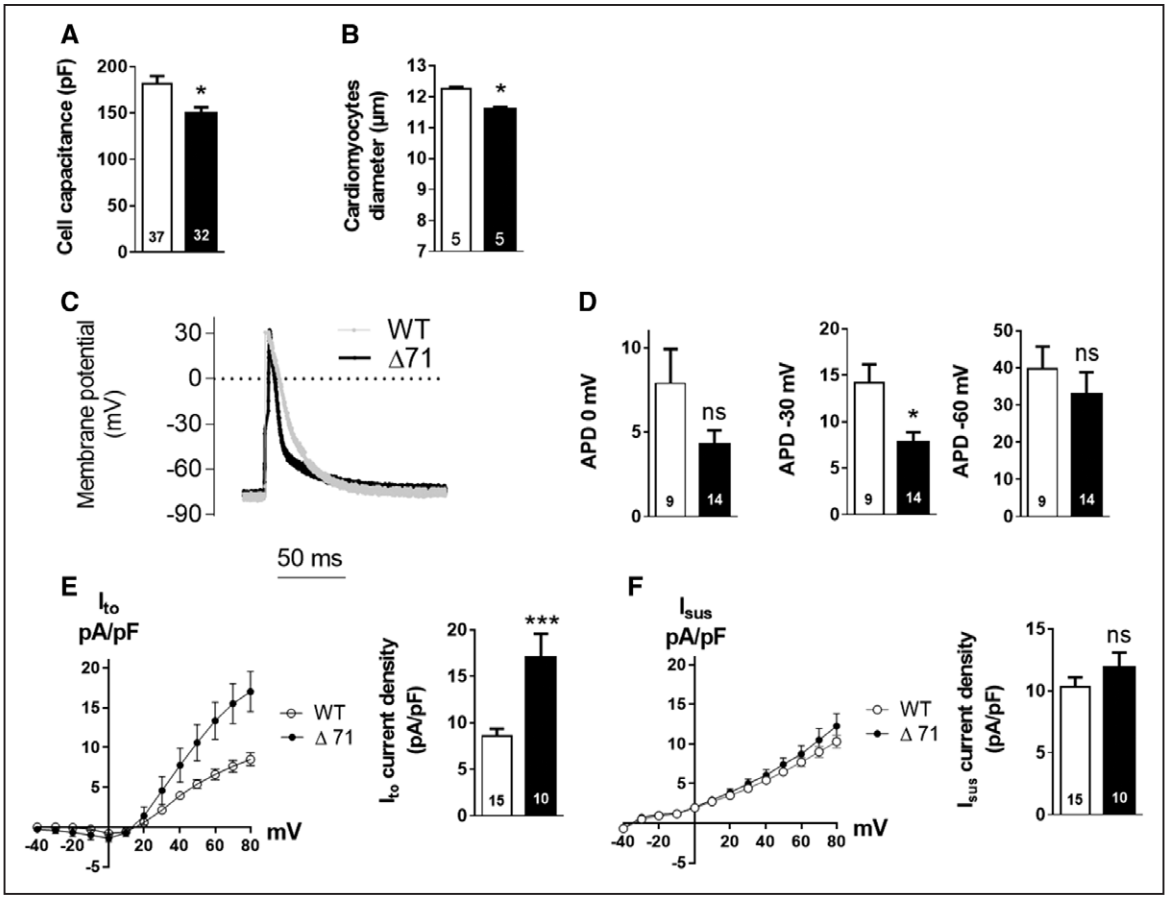

Figure 8. Bone morphogenetic protein receptor 2 (*Bmpr2*) deficiency is associated with decreased right ventricular (RV) cardiomyocytes size and action potential (AP) remodeling.

A, RV cardiomyocyte capacitance from Δ*71* and wild-type (WT) rats (32–37 cells from 3 rats). **B**, Quantification of the diameters of RV cardiomyocytes in Δ*71* and WT rats (10–15 images per animal from 3–4 rats). **C**, Representative APs in RV cardiomyocytes from Δ*71* and WT rats. **D**, Analysis of AP duration (APD) at 0-, –30-, and –60-mV membrane repolarization in Δ*71* and WT rats (9–14 cells from 3 rats). **E**, **Left**, Current-voltage relationship of transient outward-K^+ currents (I_{to}) from RV cardiomyocytes from Δ*71* and WT rats. **Right**, Average I_{to} density (10–15 cells from 3 rats). **F**, **Left**, Current-voltage relationships of sustained outward-K^+ currents (I_{sus}) from RV cardiomyocytes from Δ*71* and WT rats. **Right**, Average I_{sus} density (10–15 cells from 3 rats). ns indicates not significant. **P*<0.05; ****P*<0.001.

hypoxia-induced PH. Third, this susceptibility to SPH and induced PH was concurrent with relevant pulmonary vascular alterations, including distal muscularization, perivascular matrix remodeling, lower microvascular density, and inflammation. High levels of perivascular fibrillar collagen and pulmonary IL-6 overexpression discriminated rats that developed SPH and rats that did not develop SPH. Fourth, *Bmpr2* mutations predisposed rats to PA vasoconstriction through functional K^+ current inhibition and subsequent PASMC depolarization. Changes in KCNK3 localization may be one of the main mechanisms responsible for these effects. *Bmpr2* mutations were also found to be associated with a reduction in endothelium-dependent relaxation, which may be consistent with the major ultrastructural changes observed in the pulmonary endothelium of these rats. Finally, *Bmpr2* mutant rats showed intrinsic RV dysfunction, highlighted by PH-independent decreases in CO, RV cardiomyocyte size, and action potential duration; decreases in active tension development and sensitivity to Ca^{2+} in skinned RV cardiomyocytes; and reduced $[Ca^{2+}]_i$ transients, SR Ca^{2+} load, and cell shortening. All these alterations were observed in *Bmpr2* mutant rats without SPH. The study of these rats allowed us to delineate the primary contribution of the mutation to the phenotype independently of the alterations occurring secondary to PH and subsequent molecular and cellular activations. The former mechanisms are at the heart of PH susceptibility.

The variety of pulmonary vascular alterations that we observed in *Bmpr2*-mutant rats were consistent with recent findings related to pulmonary hemodynamic disturbances in PAH.[17] Indeed, narrowing of resistance vessels is heterogeneous, and this heterogeneous narrowing alone cannot explain the large increase in resistance in PAH. Previous studies have suggested that rarefaction could be an important contributor to the hemodynamic changes.[17] The abnormally low microvascular density observed in *Bmpr2* mutant rats during aging supported this hypothesis. Moreover, patients with PAH harboring *BMPR2* mutations are less likely to respond to acute vasodilator testing.[18] The reduction

in endothelium-dependent relaxation found in *Bmpr2*-deficient animals may partly explain this clinical observation. Increasing evidence also suggests a central role for the biochemical and biomechanical properties of the extracellular matrix in PH.[19] However, it is unclear whether extracellular matrix remodeling is merely an end-stage feature of PH or whether massive fibrosis is necessary to induce pathogenic outcomes. Numerous animal models of PH/PAH exist; however, these accelerated models of PH development make it difficult to obtain accurate insights into the pathological events. Our *Bmpr2* transgenic rat model clarified these points by allowing us to study the early development of periarteriolar fibrosis in *Bmpr2* mutant rats, even before physiological manifestation of PH (3 months of age). Furthermore, increased vascular fibrosis was markedly pronounced in *Bmpr2* mutant rats that develop SPH compared with *Bmpr2* mutant rats that did not develop SPH, suggesting a PH-dependent threshold of fibrillar collagen and resulting perivascular stiffness.[19] Taken together, these results reinforce the importance of mechanical cues in the development of cardiovascular diseases such as PH/PAH, even in genetically driven forms. Overall, our results presented a valuable model to study perivascular extracellular matrix properties during PH/PAH development.

Another valuable finding was the reduced CO observed in both *Bmpr2*-deficient rat lines from 6 months of age. Indeed, data from the Registry to Evaluate Early and Long-Term PAH Disease Management demonstrated >2-fold increases in hazard ratios for mortality among patients with hPAH compared with patients with iPAH.[20] Furthermore, RV stroke work index and cardiac index are both decreased in hPAH,[21,22] suggesting the potential impairment of RV function in this PAH subtype. Notably, Claessen and colleagues[23] have shown that humans with asymptomatic *BMPR2* mutations did not show abnormal RV contractile reserve, as measured by the change in contractility at rest and at peak exercise, even when under hypoxic conditions. Despite that, under the same conditions, the increase in RV ejection fraction is significantly lower in BMPR2 carriers while also showing decreased pulmonary arterial compliance and mean PA pressure at rest, and a close-to-significant decrease in cardiopulmonary fitness, suggesting a small degree of intrinsic RV dysfunction in these patients. Moreover, van der Bruggen et al[24] recently demonstrated, by combining in vivo measurements of RV function with molecular and histological analyses of unique RV and LV tissues from patients with PAH and controls, that despite a similar afterload, RV function is more severely compromised in *BMPR2* mutation carriers than in noncarriers. These findings suggest that *BMPR2* mutations may have a negative effect on RV function in patients with PAH. To date, differences in survival and disease severity have been explained mainly by more severe pulmonary vascular involvement, leading to a more severe and faster disease trajectory. However, because RV function is the main determinant of prognosis and disease severity and because the *BMPR2* gene is also expressed in the RV, RV function may play a role in the different clinical phenotypes of mutation carriers and noncarriers. In animals, impaired hypertrophy attributable to altered cardiac energy metabolism in the RV has been demonstrated in a transgenic mouse model expressing mutant *Bmpr2*.[25] In this study, the induced impairment of cardiomyocyte BMPRII signaling via a receptor cytoplasmic domain mutation limited the ability of the RV to undergo hypertrophy in response to increased pressure. Thus, mutant BMPRII expression in the RV may impair hypertrophic responses resulting in part from fatty acid oxidation defects. Indeed, fatty acid oxidation is the preferred energy source in cardiomyocytes.[26] Furthermore, cardiomyocytes derived from mouse embryonic stem cells mutant for either the cytoplasmic or kinase domain of BMPRII showed no increase in expression of brain natriuretic peptide in response to phenylephrine-induced hypertrophy,[27] demonstrating the incapacity to respond to hypertrophic stimuli. In fact, mice mutant for *bmpr2* show decreased exercise capacity at baseline and respond worse to pressure overload.[28] Of note, induced pluripotent stem cell–derived cardiomyocytes differentiated from patients with hPAH and *BMPR2* mutation showed decreased expression of hypertrophy-associated genes (*MYH6/7* and *ANP*), further corroborating the lack of adaptation of these cardiomyocytes, which was corrected by *BMPR2* mutation correction.[29]

Cardiomyocytes from the RV of patients with PAH were found to show increased cardiomyocyte stiffness (increased passive tension) and hypercontractility, with increases in both active tension development and improved calcium sensitivity.[30] Those mechanisms, suggested to cope for the increasing afterload imposed on the RV in PAH, seem to have been lost in our *Bmpr2* mutant rats. In contrast, decreased active tension and calcium sensitivity are associated with RV dysfunction in pressure overload[31] and could be similar to our observations in *Bmpr2* mutant rats. Indeed, we observed Ca^{2+} cycling alterations and depressed cell contractility associated with decreased calcium sensitivity for sarcomeres. Patients with systemic sclerosis–associated PAH show decreased RV functional reserve, demonstrating decreased adaption to exercise and a lack of contractility increase in response to increased load.[32] At the same time, these patients have decreased mean PAP compared with patients with iPAH[33,34] and present with lower cardiomyocyte active force development compared with both patients with iPAH and control subjects,[35] similar to our results in *Bmpr2* mutant animals. These findings, together with the fact that asymptomatic patients carrying *BMPR2* mutations show

decreased pulmonary compliance, which is further aggravated by hypoxia,[36] may explain the susceptibility of these patients to PAH with a more severe RV dysfunction. Future studies will focus on a more detailed evaluation of cardiovascular function (including PV loops and magnetic resonance imaging), which will determine to what extent the RV (and LV) of the *Bmpr2* mutant rats is compromised and will aim at determining the adaptability of these hearts to increased load.

We functionally evaluated BMPRII deficiency via the decrease in SMAD1/5/8 phosphorylation. BMPRII interacts directly with several proteins relevant to regulation of the actin cytoskeleton, including LIMK, TCTEX, and SRC.[6] Actin cytoskeleton defect is a common feature in all classes of *BMPR2* mutations found in mouse and human instances of PH/PAH.[6] Furthermore, an alternative spliced variant of *BMPR2* lacking exon 12 has been found to be overrepresented in cells from *BMPR2* mutant patients with PAH. Exon 12 forms the intracytoplasmic tail domain of BMPRII that interacts with the cytoskeleton regulatory proteins.[37] In line with these results, it is tempting to speculate that the lower PH penetrance in Δ*140* rats arising in a paradoxical more altered SMAD signaling background may be related to different cytoskeletal defects. Further investigation is needed to determine the role of actin cytoskeleton on the occurrence and severity of PAH in Δ*71* and Δ*140* rats.

Δ*71* and Δ*140* Sprague Dawley rats develop mild SPH. However, it has been demonstrated that variation in strain, even between colonies of the same strain, has a remarkable influence on the nature and severity of the response to an experimental PH trigger such as SU5416, consistent with an important role for genetic modifiers of the PAH phenotype.[38] Consistent with this concept, it was found that chronic hyperglycemia induces vascular damage predominantly in PAs, leading to PH in Wistar Kyoto but not in Sprague Dawley rats.[39] Further studies are needed to investigate the role of the genetic background on the occurrence and severity of PAH in the context of *Bmpr2* mutation.

Our model has 2 main limitations:

1. *Bmpr2* mutant female rats did not develop SPH, whereas the prevalence of iPAH and hPAH is ≈4-fold higher in women than in men.[3] Actually, this is not so surprising because there is a paradoxical opposite male bias in typical rodent models of PH (chronic hypoxia or monocrotaline); in these models, administration of estrogenic compounds (eg, estradiol-17 β) is protective (estrogen paradox).[40] This paradox is poorly understood. However, Sehgal et al[40] described an estradiol-17 β–sensitive central neuroendocrine mechanism of sex bias that culminated in species-specific male (pulsatile) versus female (more continuous) temporal patterns of circulating growth hormone (GH) levels.[40] In adult male rats, GH is released into the circulation in discrete pulses, with little or no circulating GH detectable during the interpulse interval. In female rats, the pulses are more frequent, the pulse heights are lower, and the interpulse levels are higher. In contrast, men show infrequent GH pulses of high magnitude, with very low interpulse levels; however, women show a more continuously high level of GH. On average, women have 80- to 120-fold higher levels of circulating GH than men. Thus, a difference between female humans and female rodents is the much higher continuous GH levels in women compared with female rodents. These 80- to 120-fold higher levels and a more continuous pattern of GH, and thus activation of different sets of cell cycle, cell proliferation, and cell migration regulatory genes, may explain why iPAH is more prevalent in women than men.[40] Moreover, there are significant physiological differences in hematologic and biochemical analytes between male and female Sprague Dawley rats and between rodents and humans.[41] For instance, men, premenopausal women, and postmenopausal women have similar plasma erythropoietin levels,[42] whereas erythropoietin levels in male rats are lower than in female rats.[43] Given that erythropoietin attenuates pulmonary vascular remodeling in experimental PH through interplay between endothelial progenitor cells and activation of the cytoprotective enzyme heme oxygenase-1,[44] this may underlie male susceptibility to PH in rat. Overall, factors such as genetic background, diet, temperature, hormonal cycles, metabolic rate, enzyme activities, and circadian rhythms all can influence the metabolism of an organism.[41]
2. *Bmpr2* mutated rats display variable expression of the PH phenotype. Actually, the rats used in this study have a Sprague Dawley background, which is an outbred strain. By definition, outbred strains maintain genetic variation to conserve heterozygosity within its population. Therefore, the likelihood of other mutations contributing as a second hit, promoting the development of PAH, is decreased. The entailed genetic variability associated with these rats is sufficient to change their growth rate,[45] highlighting the significant role of outbred-associated variability, and results in increased susceptibility to certain diseases when polymorphisms/mutations on specific genes are present,[46] with low penetrance,[47] similar to our own. Finally, Sprague Dawley rats hyperresponsive to vascular endothelial growth factor inhibition develop severe PH, but again with incomplete penetrance. Although 72% of male rats developed PH, only 27% of female rats developed PH. These

findings strengthen the fact that outbred strain (like the Sprague Dawley rat used in our study) can present increased susceptibility to PH as the result of a mutation, but with incomplete penetrance. Moreover, and consistent with our results, these data demonstrated that females are less prone to exhibit a phenotype.[48] Together, these findings argue in favor of the facts that the presence of the same mutation and environment contribute to the development of *BMPR2* mutation-associated SPH and that a significantly diverse genetic background, resulting from the use of an outbred species, greatly contributes to a lack of complete penetrance. Moreover, mice with endothelium-specific *Bmpr2* deletion[49] show PH development in only 20% of heterozygous mutation–carrying animals, whereas 39% of homozygous animals show increased pulmonary pressures, demonstrating that even in an inbred strain *bmpr2* mutation does not result in complete penetrance of PH.

Conclusions

Rat lines with monoallelic mutation in the *Bmpr2* gene did not develop severe PAH, but exhibited salient pathobiological features of hPAH, including similar penetrance, pulmonary vascular remodeling, and reduced microvascular density, and showed endothelial dysfunction associated with altered vasoreactivity and overactivation of mitogenic signaling pathways. Thus, these rats are valuable models for studying PAH susceptibility mechanisms related to *BMPR2* mutations. However, the slow onset (6–12 months), low incidence, and mild disease may discourage their use as a preclinical model of PAH harboring the late symptomatic clinical presentation of the human disease. Our data also showed that *Bmpr2* mutants exhibited intrinsic cardiomyocyte dysfunction, which could underscore their increased susceptibility to cardiac overload.

ARTICLE INFORMATION

Received March 8, 2018; accepted September 18, 2018.

The online-only Data Supplement is available with this article at https://www.ahajournals.org/doi/suppl/10.1161/circulationaha.118.033744.

Correspondence

Frédéric Perros, PhD, INSERM U999, Centre Chirurgical Marie Lannelongue, 133 Avenue de la Résistance, F-92350 Le Plessis Robinson, France. Email frederic.perros@inserm.fr

Affiliations

Université Paris-Sud, Faculté de Médecine, Le Kremlin-Bicêtre, France (A.H., G.M., C.R.-M., M.R., M.L., F.L., D.M., B.G., M.H., F.A., F.P.). AP-HP, Centre de Référence de l'Hypertension Pulmonaire Sévère, Département Hospitalo-Universitaire Thorax Innovation, Service de Pneumologie et Réanimation Respiratoire, Hôpital de Bicêtre, Le Kremlin-Bicêtre, France (A.H., G.M., C.R.-M., M.R., M.L., F.L., D.M., B.G., M.H., F.A., F.P.). UMRS 999, INSERM and Université Paris-Sud, Laboratoire d'Excellence en Recherche sur le Médicament et l'Innovation Thérapeutique, Le Plessis Robinson, France (A.H., G.M., C.R.-M., M.R., M.L., F.L., D.M., B.G., M.H., F.A., F.P.). Centre Chirurgical Marie Lannelongue, Le Plessis Robinson, France (A.H., G.M., C.R.-M., M.R., M.L., A.B., F.L., D.M., B.G., M.H., F.A., F.P.). Department of Surgery and Physiology, Faculty of Medicine, UnIC-Cardiovascular Research and Development Centre, University of Porto, Portugal (P.M.-F., R.A., C.B.-S.). Respiratory Division, Department of Department of Chronic Diseases, Metabolism & Aging, KU Leuven–University of Leuven, Belgium (P.M.-F.). Signalisation et Physiopathologie Cardiovasculaire, UMR-S 1180, Université Paris-Sud, INSERM, Université Paris-Saclay, 92296, Châtenay-Malabry, France (J.S., B.M., A.M.G.). Université Côte d'Azur, CNRS, IRCAN, Nice, France (T.B.). Animal Facility, Institut Paris Saclay d'Innovation Thérapeutique (UMS IPSIT), Université Paris-Sud, Université Paris-Saclay, Châtenay-Malabry, France (V.D.). Centre de Recherche de l'Institut Universitaire de Cardiologie et de Pneumologie de Québec, Laval University, QC, Canada (F.P.).

Acknowledgments

The authors thank Dr Ignacio Anegon, Laurent Tesson, and Séverine Ménoret from Transgenic Rats and Immunophenomics Core Facility (TRIP), platform TRIP–(Immunology–Nantes) for generating *Bmpr2* mutant rats. They thank the staff at the Animalerie et Exploration Fonctionnelle (AnimEx) platform for caring for the rat lines. They also thank the Microscopie et Imagerie des Micro-organismes, Animaux et Aliments (MIMA2) imaging facility (Institut national de la recherche agronomique [INRA]), Jouy-en-Josas; http://www6.jouy.inra.fr/mima2) for the transmission electron microscopy images and Christine Pechoux and Martine Letheule for excellent technical support. They thank Prof Adelino Leite-Moreira for collaboration with Cardiovascular R&D Unit (UnIC) and Naomi Kaminsky for quantifying heart capillarization. They acknowledge the support of the European Respiratory Society, Fellowship LTRF 2017 (LTRF-2017 01–00063).

Sources of Funding

Dr Perros received funding from the French National Research Agency (Agence Nationale de la Recherche, Grant ANR-13-JSV1-0011-01) and from the Fondation du Grand défi Pierre Lavoie. Dr Perros also received a Pulmonary Vascular Research Institute BMPR2 Research Grant supported by the Dinosaur Trust. Dr Hautefort is supported by a PhD grant from Région Ile de France (Domaine d'Intérêt Majeur "maladies Cardiovasculaires-Obésité-Rein-Diabète") and by the Fondation de la Recherche Médicale. G. Manaud and Dr Riou are supported by the Fonds de dotation Recherche en Santé Respiratoire. M. Lambert is supported by Therapeutic Innovation Doctoral School (Ecole Doctorale ED569). Dr Antigny receives funding from the Fondation du Souffle et Fonds de Dotation Recherche en Santé Respiratoire, Fondation Lefoulon-Delalande, and Fondation Legs Poix. Drs Mendes-Ferreira, Adão, and Brás-Silva receive funds from the European Union through the European Regional Development Fund, European Structural and Investment Funds, under Lisbon Portugal Regional Operational Program and Fundação para a Ciência e a Tecnologia (DOCnet: NORTE-01-0145-FEDER-000003; IMPAcT-PTDC/MED-FSL/31719/2017), and Drs Mendes-Ferreira and Adão are supported by Fundação para a Ciência e a Tecnologia (SFRH/BD/87714/2012 and SFRH/BD/96403/2013, respectively).

Disclosures

None.

REFERENCES

1. Hoeper MM, Bogaard HJ, Condliffe R, Frantz R, Khanna D, Kurzyna M, Langleben D, Manes A, Satoh T, Torres F, Wilkins MR, Badesch DB. Definitions and diagnosis of pulmonary hypertension. *J Am Coll Cardiol*. 2013;62(suppl):D42–D50. doi: 10.1016/j.jacc.2013.10.032
2. Guignabert C, Bailly S, Humbert M. Restoring BMPRII functions in pulmonary arterial hypertension: opportunities, challenges and limitations. *Expert Opin Ther Targets*. 2017;21:181–190. doi: 10.1080/14728222.2017.1275567
3. Mair KM, Johansen AK, Wright AF, Wallace E, MacLean MR. Pulmonary arterial hypertension: basis of sex differences in incidence and treatment response. *Br J Pharmacol*. 2014;171:567–579. doi: 10.1111/bph.12281
4. Larkin EK, Newman JH, Austin ED, Hemnes AR, Wheeler L, Robbins IM, West JD, Phillips JA, Hamid R, Loyd JE. Longitudinal analysis casts doubt on the presence of genetic anticipation in heritable pulmonary arterial hy-

pertension. *Am J Respir Crit Care Med*. 2012;186:892–896. doi: 10.1164/rccm.201205-0886OC
5. Majka S, Hagen M, Blackwell T, Harral J, Johnson JA, Gendron R, Paradis H, Crona D, Loyd JE, Nozik-Grayck E, Stenmark KR, West J. Physiologic and molecular consequences of endothelial Bmpr2 mutation. *Respir Res*. 2011;12:84. doi: 10.1186/1465-9921-12-84
6. Johnson JA, Hemnes AR, Perrien DS, Schuster M, Robinson LJ, Gladson S, Loibner H, Bai S, Blackwell TR, Tada Y, Harral JW, Talati M, Lane KB, Fagan KA, West J. Cytoskeletal defects in Bmpr2-associated pulmonary arterial hypertension. *Am J Physiol Lung Cell Mol Physiol*. 2012;302:L474–L484. doi: 10.1152/ajplung.00202.2011
7. Gomez-Arroyo J, Saleem SJ, Mizuno S, Syed AA, Bogaard HJ, Abbate A, Taraseviciene-Stewart L, Sung Y, Kraskauskas D, Farkas D, Conrad DH, Nicolls MR, Voelkel NF. A brief overview of mouse models of pulmonary arterial hypertension: problems and prospects. *Am J Physiol Lung Cell Mol Physiol*. 2012;302:L977–L991. doi: 10.1152/ajplung.00362.2011
8. Mashimo T. Gene targeting technologies in rats: zinc finger nucleases, transcription activator-like effector nucleases, and clustered regularly interspaced short palindromic repeats. *Dev Growth Differ*. 2014;56:46–52. doi: 10.1111/dgd.12110
9. Beppu H, Kawabata M, Hamamoto T, Chytil A, Minowa O, Noda T, Miyazono K. BMP type II receptor is required for gastrulation and early development of mouse embryos. *Dev Biol*. 2000;221:249–258. doi: 10.1006/dbio.2000.9670
10. Lowery JW, Intini G, Gamer L, Lotinun S, Salazar VS, Ote S, Cox K, Baron R, Rosen V. Loss of BMPR2 leads to high bone mass due to increased osteoblast activity. *J Cell Sci*. 2015;128:1308–1315. doi: 10.1242/jcs.156737
11. Tan TY, Gonzaga-Jauregui C, Bhoj EJ, Strauss KA, Brigatti K, Puffenberger E, Li D, Xie L, Das N, Skubas I, Deckelbaum RA, Hughes V, Brydges S, Hatsell S, Siao CJ, Dominguez MG, Economides A, Overton JD, Mayne V, Simm PJ, Jones BO, Eggers S, Le Guyader G, Pelluard F, Haack TB, Sturm M, Riess A, Waldmueller S, Hofbeck M, Steindl K, Joset P, Rauch A, Hakonarson H, Baker NL, Farlie PG. Monoallelic BMP2 variants predicted to result in haploinsufficiency cause craniofacial, skeletal, and cardiac features overlapping those of 20p12 deletions. *Am J Hum Genet*. 2017;101:985–994. doi: 10.1016/j.ajhg.2017.10.006
12. Humbert M, Monti G, Brenot F, Sitbon O, Portier A, Grangeot-Keros L, Duroux P, Galanaud P, Simonneau G, Emilie D. Increased interleukin-1 and interleukin-6 serum concentrations in severe primary pulmonary hypertension. *Am J Respir Crit Care Med*. 1995;151:1628–1631. doi: 10.1164/ajrccm.151.5.7735624
13. Steiner MK, Syrkina OL, Kolliputi N, Mark EJ, Hales CA, Waxman AB. Interleukin-6 overexpression induces pulmonary hypertension. *Circ Res*. 2009;104:236–244, 28p following 244. doi: 10.1161/CIRCRESAHA.108.182014
14. Tamura Y, Phan C, Tu L, Le Hiress M, Thuillet R, Jutant EM, Fadel E, Savale L, Huertas A, Humbert M, Guignabert C. Ectopic upregulation of membrane-bound IL6R drives vascular remodeling in pulmonary arterial hypertension. *J Clin Invest*. 2018;128:1956–1970. doi: 10.1172/JCI96462
15. Antigny F, Hautefort A, Meloche J, Belacel-Ouari M, Manoury B, Rucker-Martin C, Péchoux C, Potus F, Nadeau V, Tremblay E, Ruffenach G, Bourgeois A, Dorfmüller P, Breuils-Bonnet S, Fadel E, Ranchoux B, Jourdon P, Girerd B, Montani D, Provencher S, Bonnet S, Simonneau G, Humbert M, Perros F. Potassium channel subfamily K member 3 (KCNK3) contributes to the development of pulmonary arterial hypertension. *Circulation*. 2016;133:1371–1385. doi: 10.1161/CIRCULATIONAHA.115.020951
16. Bers DM. Cardiac sarcoplasmic reticulum calcium leak: basis and roles in cardiac dysfunction. *Annu Rev Physiol*. 2014;76:107–127. doi: 10.1146/annurev-physiol-020911-153308
17. Rol N, Timmer EM, Faes TJC, Vonk Noordegraaf A, Grünberg K, Bogaard H-J, Westerhof N. Vascular narrowing in pulmonary arterial hypertension is heterogeneous: rethinking resistance. *Physiol Rep*. 2017;5: e13159. doi: 10.14814/phy2.13159
18. Evans JDW, Girerd B, Montani D, Wang X-J, Galiè N, Austin ED, Elliott G, Asano K, Grünig E, Yan Y, Jing Z-C, Manes A, Palazzini M, Wheeler LA, Nakayama I, Satoh T, Eichstaedt C, Hinderhofer K, Wolf M, Rosenzweig EB, Chung WK, Soubrier F, Simonneau G, Sitbon O, Gräf S, Kaptoge S, Di Angelantonio E, Humbert M, Morrell NW. BMPR2 mutations and survival in pulmonary arterial hypertension: an individual participant data meta-analysis. *Lancet Respir Med*. 2016;4:129–137. doi: 10.1016/S2213-2600(15)00544-5
19. Dabral S, Pullamsetti SS. Vascular stiffness and mechanotransduction: back in the limelight. *Am J Respir Crit Care Med*. 2017;196:527–530. doi: 10.1164/rccm.201611-2254LE
20. Benza RL, Miller DP, Gomberg-Maitland M, Frantz RP, Foreman AJ, Coffey CS, Frost A, Barst RJ, Badesch DB, Elliott CG, Liou TG, McGoon MD. Predicting survival in pulmonary arterial hypertension: insights from the Registry to Evaluate Early and Long-Term Pulmonary Arterial Hypertension Disease Management (REVEAL). *Circulation*. 2010;122:164–172. doi: 10.1161/CIRCULATIONAHA.109.898122
21. Brittain EL, Pugh ME, Wheeler LA, Robbins IM, Loyd JE, Newman JH, Larkin EK, Austin ED, Hemnes AR. Shorter survival in familial versus idiopathic pulmonary arterial hypertension is associated with hemodynamic markers of impaired right ventricular function. *Pulm Circ*. 2013;3:589–598. doi: 10.1086/674326
22. Girerd B, Montani D, Eyries M, Yaici A, Sztrymf B, Coulet F, Sitbon O, Simonneau G, Soubrier F, Humbert M. Absence of influence of gender and BMPR2 mutation type on clinical phenotypes of pulmonary arterial hypertension. *Respir Res*. 2010;11:73. doi: 10.1186/1465-9921-11-73
23. Claessen G, La Gerche A, Petit T, Gillijns H, Bogaert J, Claeys M, Dymarkowski S, Claus P, Delcroix M, Heidbuchel H. Right ventricular and pulmonary vascular reserve in asymptomatic BMPR2 mutation carriers. *J Heart Lung Transplant*. 2017;36:148–156. doi: 10.1016/j.healun.2016.06.018
24. van der Bruggen CE, Happé CM, Dorfmüller P, Trip P, Spruijt OA, Rol N, Hoevenaars FP, Houweling AC, Girerd B, Marcus JT, Mercier O, Humbert M, Handoko ML, van der Velden J, Vonk Noordegraaf A, Bogaard HJ, Goumans MJ, de Man FS. Bone morphogenetic protein receptor type 2 mutation in pulmonary arterial hypertension: a view on the right ventricle. *Circulation*. 2016;133:1747–1760. doi: 10.1161/CIRCULATIONAHA.115.020696
25. Hemnes AR, Brittain EL, Trammell AW, Fessel JP, Austin ED, Penner N, Maynard KB, Gleaves L, Talati M, Absi T, Disalvo T, West J. Evidence for right ventricular lipotoxicity in heritable pulmonary arterial hypertension. *Am J Respir Crit Care Med*. 2014;189:325–334.
26. Lopaschuk GD, Ussher JR, Folmes CD, Jaswal JS, Stanley WC. Myocardial fatty acid metabolism in health and disease. *Physiol Rev*. 2010;90:207–258. doi: 10.1152/physrev.00015.2009
27. Talati M, Funke M, Bylund J, Trammell A, Majka S, Fessel J, West J, Newman J, Hatzopoulos A, Hemnes A. Mutant BMPR2 expression in cardiomyocytes results in an altered hypertrophic response (1090.2). *FASEB J*. 2014;28:1090.2.
28. Boehm M, Tian X, Zhao M, Dannewitz S, Kuramoto K, Kuang J, Reddy S, Bernstein D, Ashley E, Spiekerkoetter E. Reduced BMPR2 Signaling Impairs Right Ventricular Heart Function and Exaggerates Cardiac Fibrosis Upon Chronic Pressure Overload. *Am J Respir Crit Care Med*. 2017;195:A5112.
29. Kuramoto K, Boehm M, Tian X, Dannewitz S, Gu M, Silin S, Seeger T, Kitani T, Wu JC, Rabinovitch M, Spiekerkoetter E. Reduced BMPR2 Signaling Alters the Expression of Hypertrophy Related Genes in Induced Pluripotent Stem Cell Derived Cardiomyocytes of PAH Patients. *Am J Respir Crit Care Med* 2018;197:A3754.
30. Rain S, Handoko ML, Trip P, Gan CT, Westerhof N, Stienen GJ, Paulus WJ, Ottenheijm CA, Marcus JT, Dorfmüller P, Guignabert C, Humbert M, Macdonald P, Dos Remedios C, Postmus PE, Saripalli C, Hidalgo CG, Granzier HL, Vonk-Noordegraaf A, van der Velden J, de Man FS. Right ventricular diastolic impairment in patients with pulmonary arterial hypertension. *Circulation*. 2013;128:2016–2025, 1–10. doi: 10.1161/CIRCULATIONAHA.113.001873
31. Mendes-Ferreira P, Santos-Ribeiro D, Adão R, Maia-Rocha C, Mendes-Ferreira M, Sousa-Mendes C, Leite-Moreira AF, Brás-Silva C. Distinct right ventricle remodeling in response to pressure overload in the rat. *Am J Physiol Heart Circ Physiol*. 2016;311:H85–H95. doi: 10.1152/ajpheart.00089.2016
32. Hsu S, Houston BA, Tampakakis E, Bacher AC, Rhodes PS, Mathai SC, Damico RL, Kolb TM, Hummers LK, Shah AA, McMahan Z, Corona-Villalobos CP, Zimmerman SL, Wigley FM, Hassoun PM, Kass DA, Tedford RJ. Right ventricular functional reserve in pulmonary arterial hypertension. *Circulation*. 2016;133:2413–2422. doi: 10.1161/CIRCULATIONAHA.116.022082
33. Tedford RJ, Mudd JO, Girgis RE, Mathai SC, Zaiman AL, Housten-Harris T, Boyce D, Kelemen BW, Bacher AC, Shah AA, Hummers LK, Wigley FM, Russell SD, Saggar R, Saggar R, Maughan WL, Hassoun PM, Kass DA. Right ventricular dysfunction in systemic sclerosis-associated pulmonary arterial hypertension. *Circ Heart Fail*. 2013;6:953–963. doi: 10.1161/CIRCHEARTFAILURE.112.000008
34. Overbeek MJ, Lankhaar JW, Westerhof N, Voskuyl AE, Boonstra A, Bronzwaer JG, Marques KM, Smit EF, Dijkmans BA, Vonk-Noordegraaf A. Right ventricular contractility in systemic sclerosis-associated and idiopathic pulmonary arterial hypertension. *Eur Respir J*. 2008;31:1160–1166. doi: 10.1183/09031936.00135407
35. Hsu S, Kirk JA, Mullin CJ, Mukherjee M, Kolb TM, Damico RL, Mathai SC, Shah AA, Wigley FM, Margulies KB, Hassoun PM, Tedford RJ, Kass DA. Right Ven-

tricular Myofilament Functional Differences in Humans With Systemic Sclerosis–Associated Versus Idiopathic Pulmonary Arterial Hypertension. *Circulation*. 2018;137:2360–2370. doi: 10.1161/CIRCULATIONAHA.117.033147
36. Pavelescu A, Vanderpool R, Vachiéry JL, Grunig E, Naeije R. Echocardiography of pulmonary vascular function in asymptomatic carriers of BMPR2 mutations. *Eur Respir J*. 2012;40:1287–1289. doi: 10.1183/09031936.00021712
37. Cogan J, Austin E, Hedges L, Womack B, West J, Loyd J, Hamid R. Role of BMPR2 alternative splicing in heritable pulmonary arterial hypertension penetrance. *Circulation*. 2012;126:1907–1916. doi: 10.1161/CIRCULATIONAHA.112.106245
38. Jiang B, Deng Y, Suen C, Taha M, Chaudhary KR, Courtman DW, Stewart DJ. Marked strain-specific differences in the SU5416 rat model of severe pulmonary arterial hypertension. *Am J Respir Cell Mol Biol*. 2016;54:461–468. doi: 10.1165/rcmb.2014-0488OC
39. De Jesus L, Zurita E, Gomez M de J, Suarez J. Different susceptibility to vascular damage induced by chronic hyperglycemia in aortic and pulmonary arteries from Sprague Dawley and Wistar Kyoto rats. *FASEB J*. 2015;29:964. https://www.fasebj.org/doi/abs/10.1096/fasebj.29.1_supplement.964.7. Accessed January 9, 2018.
40. Sehgal PB, Yang Y-M, Miller EJ. Hypothesis: neuroendocrine mechanisms (hypothalamus-growth hormone-STAT5 axis) contribute to sex bias in pulmonary hypertension. *Mol Med Camb Mass*. 2015;21:688–701. doi: 10.2119/molmed.2015.00122
41. He Q, Su G, Liu K, Zhang F, Jiang Y, Gao J, Liu L, Jiang Z, Jin M, Xie H. Sex-specific reference intervals of hematologic and biochemical analytes in Sprague-Dawley rats using the nonparametric rank percentile method. *PLoS One*. 2017;12:e0189837. doi: 10.1371/journal.pone.0189837
42. Murphy WG. The sex difference in haemoglobin levels in adults: mechanisms, causes, and consequences. *Blood Rev*. 2014;28:41–47. doi: 10.1016/j.blre.2013.12.003
43. Kong WN, Niu QM, Ge L, Zhang N, Yan SF, Chen WB, Chang YZ, Zhao SE. Sex differences in iron status and hepcidin expression in rats. *Biol Trace Elem Res*. 2014;160:258–267. doi: 10.1007/s12011-014-0051-3
44. van Loon RL, Bartelds B, Wagener FA, Affara N, Mohaupt S, Wijnberg H, Pennings SW, Takens J, Berger RM. Erythropoietin attenuates pulmonary vascular remodeling in experimental pulmonary arterial hypertension through interplay between endothelial progenitor cells and heme oxygenase. *Front Pediatr*. 2015;3:71. doi: 10.3389/fped.2015.00071
45. Brower M, Grace M, Kotz CM, Koya V. Comparative analysis of growth characteristics of Sprague Dawley rats obtained from different sources. *Lab Anim Res*. 2015;31:166–173. doi: 10.5625/lar.2015.31.4.166
46. Kudo T, Asano J, Shimizu T, Nanashima N, Fan Y, Akita M, Ookawa K, Hayakari M, Yokoyama Y, Suto K, Tsuchida S. Different susceptibility to peroxisome proliferator-induced hepatocarcinogenesis in rats with polymorphic glutathione transferase genes. *Cancer Sci*. 2006;97:703–709. doi: 10.1111/j.1349-7006.2006.00247.x
47. Rijkers K, Mescheriakova J, Majoie M, Lemmens E, van Wijk X, Philippens M, Van Kranen-Mastenbroek V, Schijns O, Vles J, Hoogland G. Polymorphisms in CACNA1E and Camk2d are associated with seizure susceptibility of Sprague-Dawley rats. *Epilepsy Res*. 2010;91:28–34. doi: 10.1016/j.eplepsyres.2010.06.006
48. Chaudhary KR, Deng Y, Yang A, Cuppen E, Stewart DJ. A novel mutation in Hif1α in Sprague Dawley rats is associated with hyper-responsiveness to Su5416 and severe pulmonary arterial hypertension [abstract]. *Circulation*. 2016;134:A20172.
49. Hong KH, Lee YJ, Lee E, Park SO, Han C, Beppu H, Li E, Raizada MK, Bloch KD, Oh SP. Genetic ablation of the BMPR2 gene in pulmonary endothelium is sufficient to predispose to pulmonary arterial hypertension. *Circulation*. 2008;118:722–730. doi: 10.1161/CIRCULATIONAHA.107.736801